AUT Journal of Mechanical Engineering

AUT J. Mech. Eng., 3(1) (2019) 25-32
DOI: 10.22060/mej.2017.11920.5555

Numerical Investigation of Water/Al_2O_3 Nanofluid Dryout Phenomenon in a Vertical Channel

A. Rabiee*, A. Atf

School of Mechanical Engineering, Shiraz University, Shiraz, Iran

ABSTRACT: Critical heat flux (CHF) has been recognized as the upper limit for the safe operation of many cooling systems which may lead to the occurrence of dryout causing a large temperature gradient in the heated wall. One way to increase the amount of the CHF is to put in nanoparticles such as Al_2O_3 to the base fluid. The current research investigates the nanoparticles effect on dryout phenomenon using computational fluid dynamics. Boiling phenomena are simulated using the mechanistic model organized in Rensselaer Polytechnic Institute (RPI) which is extended to analyze the CHF by partitioning wall heat flux to liquid and vapor phases. It was shown that the addition of Al_2O_3 nanoparticles, postpones the wall temperature jump and the liquid temperature and the vapor volume fraction increase regularly in spite of the wall temperature jump. In another effort in this study, it was shown that the dryout phenomenon can be delayed by increasing the nanoparticles concentration, and in certain concentration of nanoparticles (5 percent), dry out would not take place. It can be concluded from obtained results that the addition of Al_2O_3 nanoparticles, delays the CHF phenomenon and therefore the safety margins of the operation would be enhanced.

Review History:

Received: 20 July 2017
Revised: 3 October 2017
Accepted: 30 October 2017
Available Online: 1 December 2017

Keywords:

Critical heat flux
Alumina nanoparticle
Dryout
Two phase
Heat Transfer

1- Introduction

Nucleate boiling is the most efficient heat transfer mechanism because of its high performance due to latent heat transfer to improve the thermal performance of components for the process industry and power plants. Therefore, boiling heat transfer has played an important role in industrial heat transfer processes such as macroscopic heat transfer exchangers in nuclear and fossil power plants. However, for the incorporation of nucleate boiling in most practical applications, it is imperative that Critical Heat Flux (CHF) is not exceeded. CHF phenomenon is the thermal limit during a heat transfer phase change; at the CHF point the heat transfer is maximized, followed by a drastic degradation after the CHF point. For decades, researchers have been trying to develop more efficient heat transfer process, and also increase the CHF. To serve this purpose, nanofluids have been employed in several experimental facilities.

In this research, alumina nanoparticles effect with various concentrations on critical heat flux phenomenon in a boiling flow filed is investigated using Computational Fluid Dynamics (CFD). The studies carried out in this context are determined in the following.

Bartolemi et al. [1] in 1969 conducted an experiment to simulate boiling flow in a vertical pipe. In this study, wall and fluid temperatures accompanied by the vapor volume fraction were measured.

Hoyer [2] in 1998 organized an experimental setup on boiling flow while the dryout phenomenon occurred due to high heat flux. It was shown that a vapor film forms around the pipe wall. Besides experimental activities, Krepper et al. [3] in 2006 showed the CFD code capability to model the two-phase boiling flows. They examined a subcooled boiling flow in a vertical channel and demonstrated that the heat partitioning model along with the rest of the flow field equations has the ability to compute the dryout phenomenon location. Good agreement with experimental data was observed. Li. et al. [4] in 2010 examined boiling flow field in a vertical pipe using Rensselaer Polytechnic Institute (RPI) model, using the FLUENT software.

Li et al. [5] in 2011 simulated the boiling phenomenon as well as the CHF phenomenon in a vertical pipe using the CFD code. They investigated the occurrence of the dryout phenomenon by adjusting the wall heat flux partitioning. The results were in relatively good agreement with experimental data.

In addition to the researches that have been performed to investigate the boiling flow field, there are numerous activities that investigated the influence of nanoparticles on boiling fluid flows.

Corcione [6] in 2011 obtained two empirical correlations to predict the effects of nanoparticles on thermal conductivity and dynamic viscosity using available experimental data in the literature. It was expressed that the thermal conductivity of the nanofluid in comparison with the base liquid was promoted by increasing the nanoparticle volume fraction.

Heyhat et al. [7] in 2013 conducted an experimental setup to investigate the alumina nanoparticles effect on the convective heat transfer coefficient. It was observed that the heat transfer coefficient would be increased by approximately 32% at 2 percent volumetric concentration of nanoparticles.

Prajapati et al. [8] in 2014 experimentally examined ZnO/water nanofluid with volume concentration of the nanoparticles varying from 0.0001 to 0.1% in a boiling flow. They observed that with the nanoparticles being more deposited on the heated surface, is increased and thus enhances the convective heat transfer.

Atf et al. [9] in 2014 investigated subcooled flow boiling accompanied by Alumina nanoparticles numerically. They

Corresponding author, E-mail: rabiee@shirazu.ac.ir

showed that adding alumina nanoparticles enhances the heat transfer coefficients.

Abedinia et al. [10] in 2017 numerically simulated the flow boiling of alumina/water nanofluid employing the mixture model. In addition to studies that have been taken place on the enrichment of nanofluid thermal conductivity, further investigations have been performed on the nanoparticles effects and inducing excessive fluctuations such as Brownian motion on the flow field [11,12].

Based on available researches, there are a small number of activities about nanofluid boiling flow accompanied by dryout. Therefore in this research tries to evaluate the capability of the CFD software. The details of numerical method are explained in the following.

2- Simulation of Boiling Flow

The boiling flow field can be studied with a variety of techniques. In order to model the boiling flow field, the following assumptions have been listed:

- Reynolds Averaged Navier-Stokes (RANS) equations for each phase have been employed with an Eulerian-Eulerian approach to determine boiling phenomenon. The nanoparticles effect was simulated by averaging the thermophysical properties.
- Boiling phenomenon is modeled by the use of the mechanistic.

2- 1- Governing equations

The governing equations for each phase in a generalized arrangement besides the required relations have been represented [4].

Continuity equation

$$\frac{\partial\left(\alpha_q\rho_q\right)}{\partial t}+\nabla\bullet\left(\alpha_q\rho_q\mathrm{V}_q\right)=\sum_{r=1}^{n}\left(\dot{m}_{rq}-\dot{m}_{qr}\right)+s_q \tag{1}$$

Momentum equation

$$\frac{\partial\left(\alpha_q\rho_q\mathbf{V}_q\right)}{\partial t}+\nabla\bullet\left(\alpha_q\rho_q\mathbf{V}_q\mathbf{V}_q\right)=-\alpha_q\nabla p+\nabla\bullet\left(\overline{\overline{\tau}}_q\right)+\alpha_q\rho_q\mathbf{B}_f$$
$$+\sum_{r=1}^{n}\left(\mathbf{F}_{rq}^{D}+\mathbf{F}_{rq}^{TD}+\dot{m}_{rq}\mathbf{V}_{rq}-\dot{m}_{qr}\mathbf{V}_{qr}\right)+\left(\mathbf{F}_q+\mathbf{F}_q^{L}+\mathbf{F}_q^{vm}\right) \tag{2}$$

Energy equation

$$\frac{\partial\left(\alpha_q\rho_qH_q\right)}{\partial t}+\nabla\bullet\left(\alpha_q\rho_q\mathbf{V}_qH_q\right)=\overline{\overline{\tau}}_q:\nabla\bullet\mathbf{V}_q$$
$$+\alpha_q\frac{\partial p}{\partial t}-\nabla\bullet\dot{\mathbf{q}}+S_{H,q}+\sum_{r=1}^{n}\left(\dot{q}_{rq}+\dot{m}_{rq}H_{rq}-\dot{m}_{qr}H_{qr}\right) \tag{3}$$

Turbulence modeling

$$\frac{\partial(\alpha_q\rho_q\phi_q)}{\partial t}+\nabla\bullet(\alpha_q\rho_q\mathbf{V}_q\phi_q)=\nabla\bullet(\alpha_q\Gamma_{\phi,q}\nabla\phi_q)+\alpha_qS_{q,\phi} \tag{4}$$

2- 2- Wall boiling models

The wall boiling has been simulated based on RPI model [13]. In this approach, total heat flux from wall to liquid as shown in Fig. 1 is divided into three parts: liquid phase convective heat flux, $\dot{q}_c$, quenching heat flux, $\dot{q}_Q$ and evaporation heat flux, $\dot{q}_E$.

$$\dot{q}_W=\dot{q}_c+\dot{q}_Q+\dot{q}_E \tag{5}$$

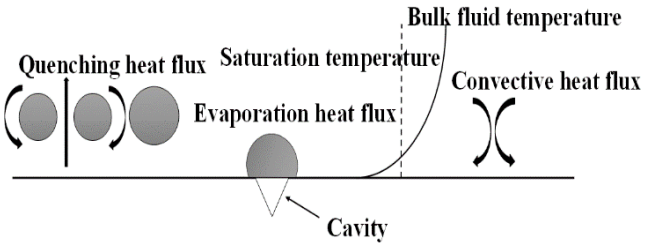

Fig. 1. A Schematic of different wall heat flux partitioning

Liquid phase convective heat flux

$$\dot{q}_c=h_C\left(T_w-T_l\right)\left(1-A_b\right) \tag{6}$$

where h_C is indicated as the liquid phase HTC.

Area of influence

$$A_b=\min\left(1,\eta\frac{\pi}{4}d_b^2N_w\right) \tag{7}$$

$$ç=4.8\exp(-\frac{Ja}{80}) \tag{8}$$

$$Ja=\frac{\rho_lC_{p,l}\Delta T_{sub}}{\rho_vH_{lv}} \tag{9}$$

Quenching heat flux

Quenching heat flux is determined as the following equation [4]:

$$\dot{q}_Q=C_{wt}\frac{2k_l}{\sqrt{\frac{\pi\gamma_l}{f_{bw}}}}\left(T_w-T_{l,q}\right)A_b \tag{10}$$

Evaporation heat flux

Evaporation heat flux is calculated by the following relation [4]:

$$q_E=\frac{\pi}{6}d_{bw}^3f_{bw}N_w\rho_vH_{lv} \tag{11}$$

Nucleation site density

Nucleation site density based on Lemmert-Chawla correlation is [16,17]:

$$N_w=C^n\left(T_w-T_{sat}\right) \tag{12}$$

Here by default, C=15545.54 and n=1.805.

Bubble departure diameter

Bubble departure diameter is modeled based on Tolubinski correlation [18,19]:

$$D_w = \min\left(0.0014, 0.0006\exp\left(-\frac{\Delta T_w}{45}\right)\right) \quad (13)$$

In order to be able to model dryout phenomenon, it is necessary to include the vapor temperature. Thus, the wall heat partition is modified as follows [4,20-21]:

$$\dot{q}_W = (\dot{q}_c + \dot{q}_Q + \dot{q}_E + \dot{q}_F) f(\alpha_l) + (1 - f(\alpha_l))\dot{q}_v + \dot{q}_G \quad (14)$$

The function $f(\alpha_v)$ based on Ioilev relation in terms of the local vapor volume is [20]:

$$f(\alpha_v) = 1 - f(\alpha_l) = \max\left(0, \min\left\{1, \frac{\alpha_v - \alpha_{v,1}}{\alpha_{v,2} - \alpha_{v,1}}\right\}\right) \quad (15)$$

2- 3- Nanofluid properties

In this research, Eqs. (16) to (19) have been used to achieve thermophysical averaged properties of the nanofluid [22-24].

$$\rho_{nf} = (1-\varphi)\rho_b + \varphi\rho_p \quad (16)$$

$$(\rho c_p)_{nf} = (1-\varphi)(\rho c_p)_{bf} + \varphi(\rho c_p)_p \quad (17)$$

$$\mu_{nf} / \mu_{bf} = 123\varphi^2 + 7.3\varphi + 1 \quad (18)$$

$$k_{nf} / k_{bf} = 4.97\varphi^2 + 2.72\varphi + 1 \quad (19)$$

Table 1 and Fig. 2 depict some thermophysical properties of nanoparticle Al_2O_3.

Table 1. Thermophysical properties of nanoparticle

Density (kg/m³)	Specific heat capacity (J/kg K)	Thermal conductivity (W/m K)
3880	773	36

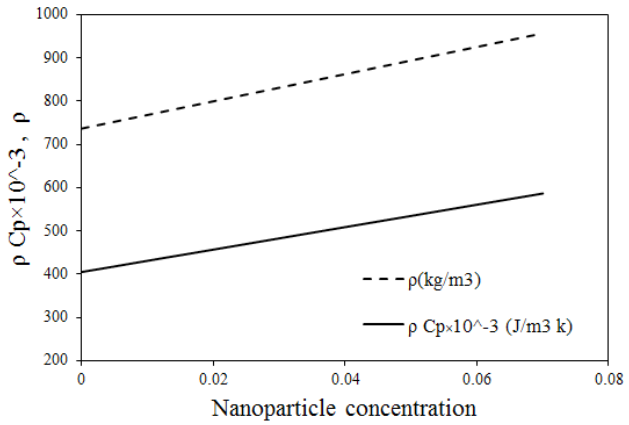

Fig. 2. Density and specific heat in terms of nanoparticles concentration

3- Results

This section determines some results including the simulation of the subcooled boiling, dryout phenomenon and the Al_2O_3 nanoparticles effects in the flow field.

3- 1- Results of subcooled boiling flow

The first case is upward subcooled boiling flow, experimentally studied by Bartolemei [1]. Fig. 3 depicts a schematic of the pipe with boundary conditions and the problem is simulated as axisymmetric and steady-state.

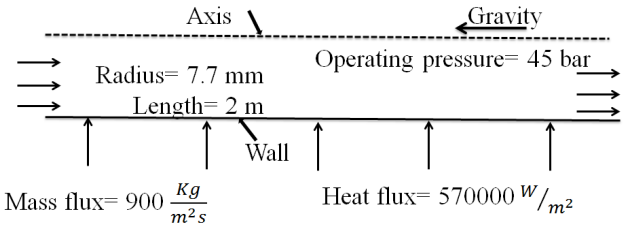

Fig. 3. Geometry and flow conditions

Fig. 4 shows the grid for numerical simulation of the current case.

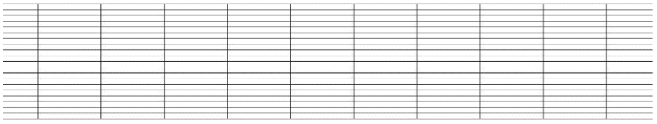

Fig. 4. Enlargement of grid generation

To study the grid independency of the solution, structured grids with 13125 and 52500 cells, were utilized. Fig. 5 depicts wall temperature for these two meshes. As can be seen from this figure, two grids go back almost alike solutions.

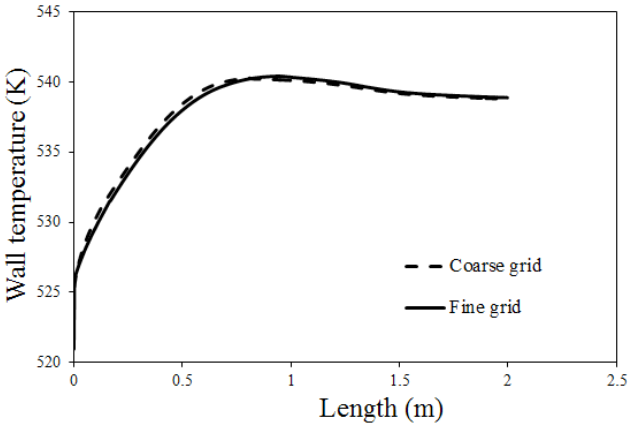

Fig. 5. Examination of grid-independence

Fig. 6 depicts the liquid temperature for different turbulence models. As can be seen the *k-ω* model is better model in this current with respect to the experimental data.

Figs. 7 to 9 shows comparisons between the computations and experimental data. Reasonable agreement between results can be seen.

Fig. 10 shows the wall heat flux partitioning including liquid phase, evaporation and quenching heat fluxes.

3- 2- CHF in vertical pipe

In this part, the results of the dryout phenomenon have been determined. The boundary condition and geometric configuration are selected from the paper by Hoyer [2]. Fig. 11 a schematic of the pipe with boundary conditions.

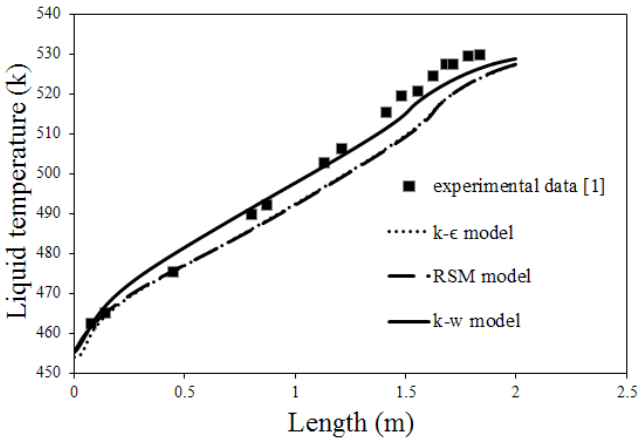

Fig. 6. Liquid temperature along the channel

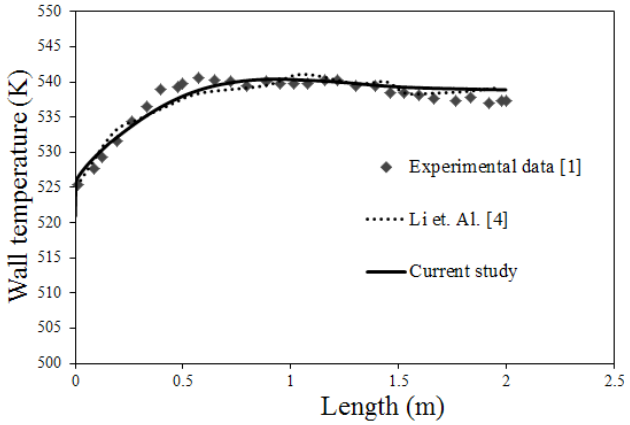

Fig. 7. Wall temperature along the channel

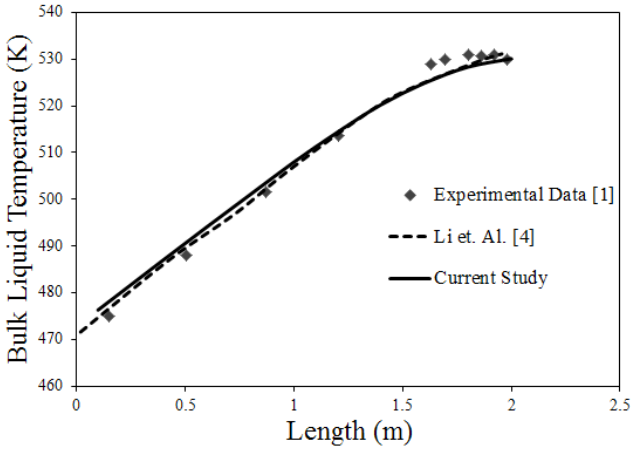

Fig. 8. Bulk liquid temperature inside the channel

Fig. 12 shows comparisons between the computations and experimental data. As can be seen, a sudden change in wall temperature has taken place.

Fig. 13 represents wall heat flux partitioning including vapor phase, evaporation and quenching heat fluxes.

Figs. 14 and 15 depict liquid and vapor velocities at the sections, 3, 5 meters.

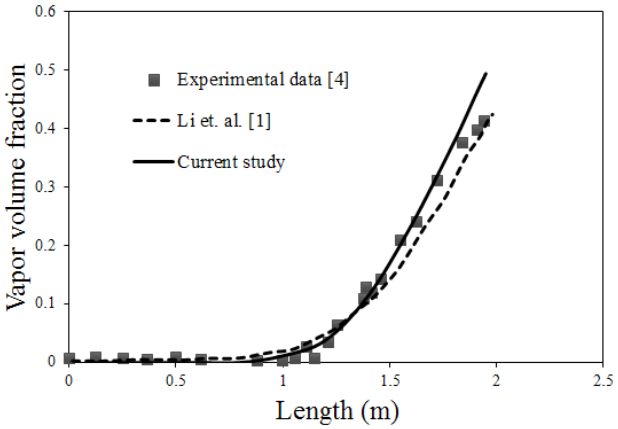

Fig. 9. Area-averaged vapor volume fraction inside the channel

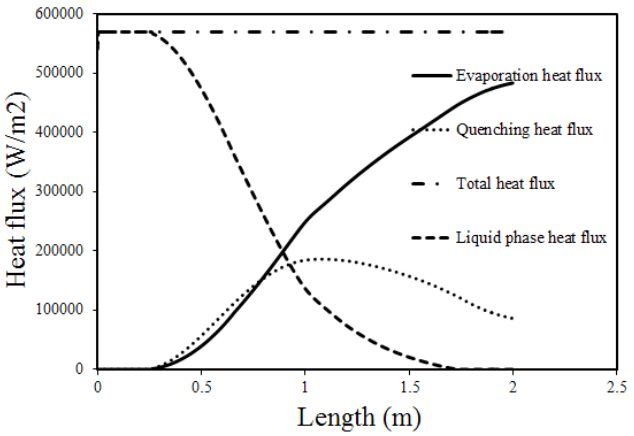

Fig. 10. Computed wall heat flux partitions

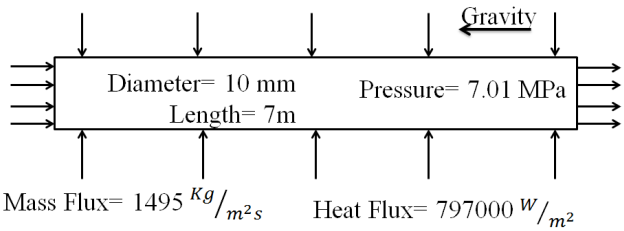

Fig. 11. Geometry and flow conditions at CHF

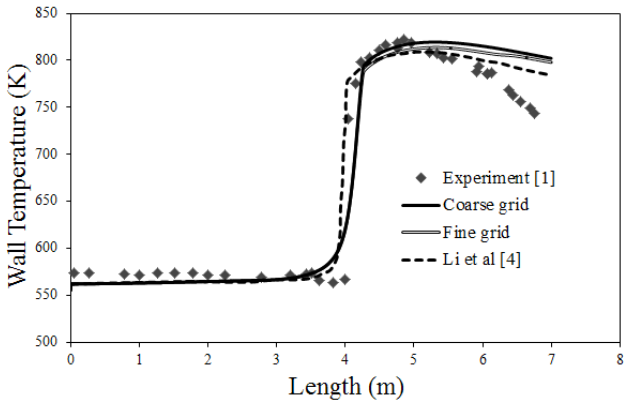

Fig. 12. Wall temperature along the channel wall

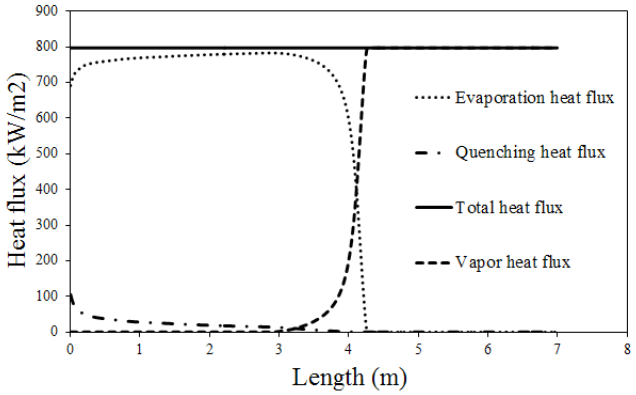

Fig. 13. Heat flux partitions for the CHF condition

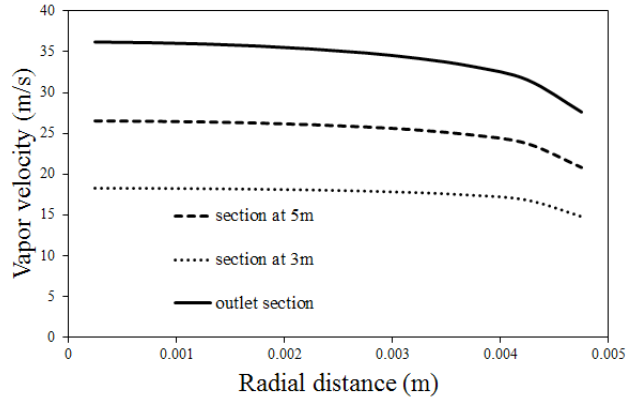

Fig. 14. Radial vapor velocity at different cross sections along the channel

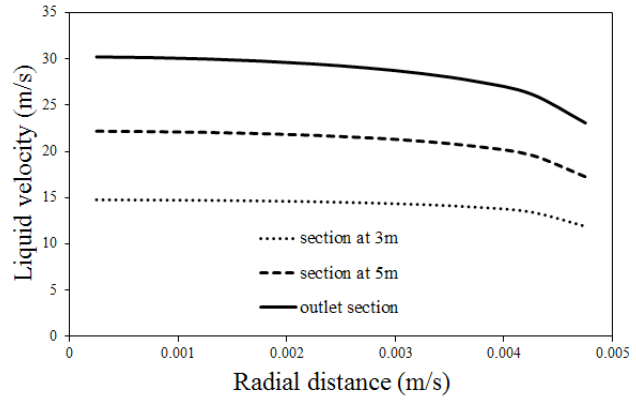

Fig. 15. Radial liquid velocity at different cross sections along the channel

3- 3- CHF in vertical pipe in the presence of Al_2O_3 nanoparticles

In the previous section, it was shown that by applying the wall heat flux equal to 797000 W/m^2 , CHF took place in the surrounding area of 4 meters from the inlet. In this part, it is tried to improve CHF threshold by adding Al_2O_3 nanoparticles. Fig. 16 depicts wall temperature with the presence of 2 percent volumetric concentration of nanoparticles for fine and coarse grid (21000, and 84000 cells) to study of grid independency of solution.

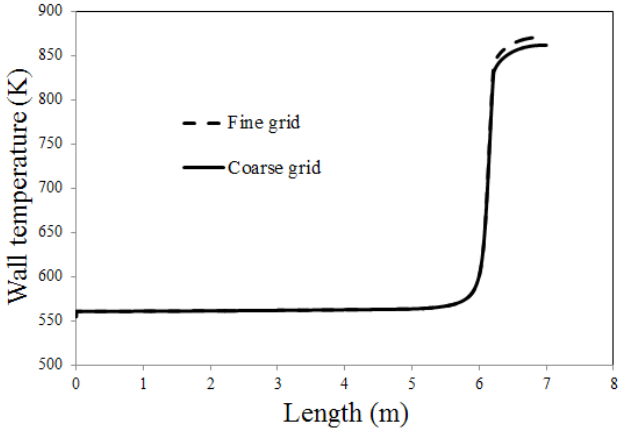

Fig. 16. Examination of grid-independence in the presence of 2 vol. % of nanoparticles

The influence of Al_2O_3 nanoparticle concentrations is depicted in Fig. 17. It can be seen that jump in the wall temperature will be delayed by the increase in the nanoparticles concentration.

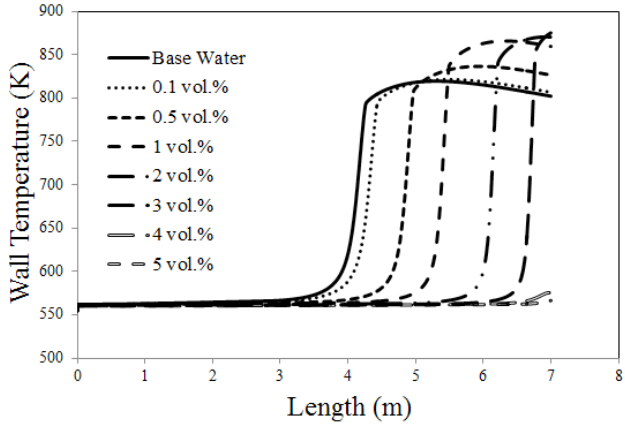

Fig. 17. Influence of nanoparticle concentration

The independence of the wall temperature on different turbulent modeling approach, dispersed, mixture and per phase is depicted in Fig. 18 with nanoparticle concentration 2 percent. It is obvious that the models have no significant effect on the results.

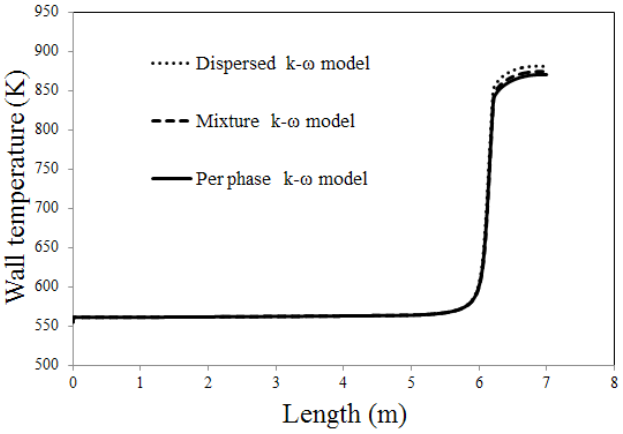

Fig. 18. Effect of different turbulent models

Figs. 19 and 20 show the bulk and axial liquid temperatures with the enhancement of the nanoparticle concentrations, respectively. It is obvious that with increasing the nanoparticles concentration, there would be a delay of the liquid temperature to reach the saturation condition.

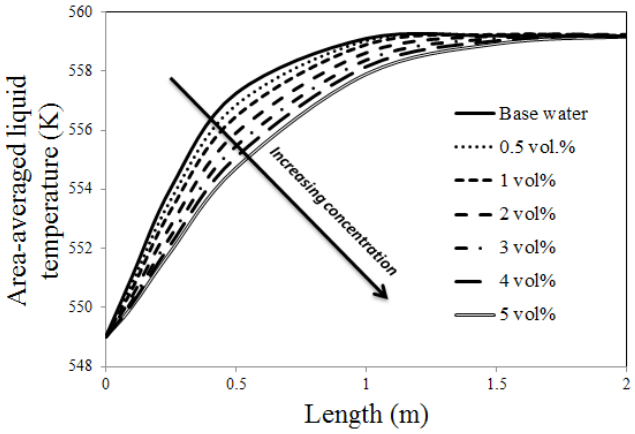

Fig. 19. Area-averaged liquid temperature with nanoparticle concentrations

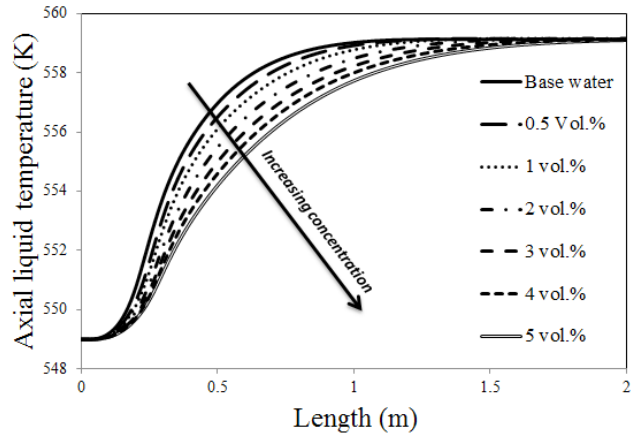

Fig. 20. Axial liquid temperature

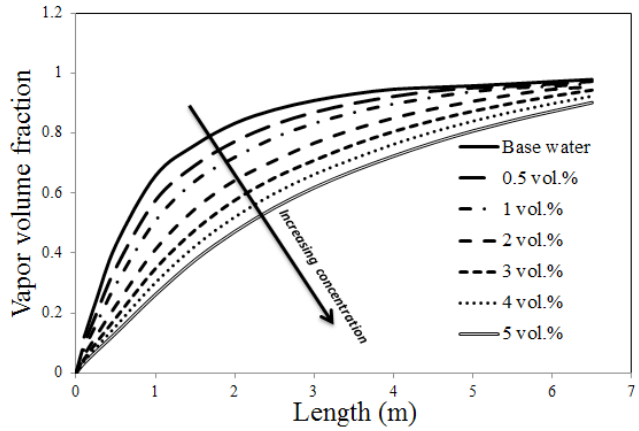

Fig. 21. Distribution of vapor volume fraction

Fig. 22. Depicts the influence of nanoparticle concentrations on the HTC. As can be seen, HTC falls down rapidly after dryout formation.

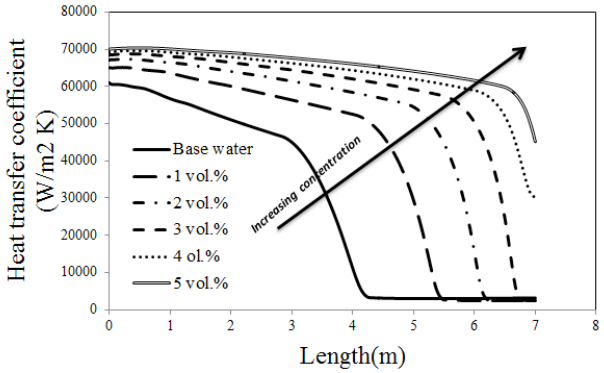

Fig. 22. Effect of various nanoparticle concentrations on HTC distribution

As seen from Fig. 17, due to the increase of nanoparticle concentration, the jump in the wall temperature has been delayed. Increasing the concentration of nanoparticles equal to 5 percent leads to that the sudden rise in the wall temperature will not occur. In another work, to find out the critical heat flux in 5 vol. %, the amount of heat flux has been improved. It is notable that by considering this amount of nanoparticles with the wall heat flux equal to 797 kW/m^2, the dryout phenomenon will not occur.

Fig. 23 depicts the influence of rising the heat flux up to 1 millionW/m^2 . As can be seen from this figure, the heat flux with the magnitude of 900 kW/m^2 , leads to temperature jump near the outlet. It is revealed that by adding nanoparticles with 5 vol. %, the CHF threshold enhances by 13 percent.

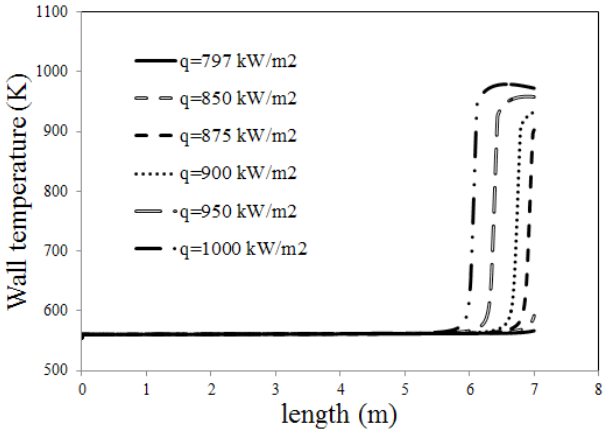

Fig. 23. Wall temperature distribution

4- Conclusion

- In this study, the influence of the addition of Al_2O_3 nanoparticles to the boiling flow accompanied by dryout phenomenon has been investigated. Boiling phenomenon is simulated using the RPI mechanistic model which can utilized to analyze the CHF by partitioning wall heat flux to liquid and vapor phases.
- It was shown that the addition of Al_2O_3 nanoparticles, postpones the wall temperature jump.
- It is concluded that the liquid temperature and the vapor volume fraction increase regularly in spite of the wall temperature jump.
- Increasing the concentration of nanoparticles equal

to 5 percent leads to that the sudden rise in the wall temperature will not occur

- It can be concluded from results that the addition of Al_2O_3 nanoparticles, delays the dryout phenomenon and therefore the safety margins of the operation would be enhanced.

References

[1] G. G. Bartolemei, V. M. Chanturiya, Experimental study of true void fraction when boiling subcooled water in vertical tubes, *Teploenergeika*, 14(2) (1969) 123-128.

[2] N. Hoyer, Calculation of dryout and post-dryout heat transfer for tube geometry, *Int. J. Multiphase Flow*, 24(1998) 319-334.

[3] E. Krepper, B. Koncar, Y. Egorov, *CFD modeling of subcooled boiling-Concept, validation and application to fuel assembly design*, Forschungszentrum Rossendorf e.V.(FZR) Germany 2006,.

[4] H. Li, S. A. Vasquez, H. Puneka, Prediction of Boiling and Critical Heat Flux Using an Eulerian Multiphase Boiling Model, *Proceedings of the ASME* 2010, *International Mechanical Engineering Congress & Exposition* 2010, canada

[5] H. Li, H. Punekar, S. A. Vasquez, R. Muralikrishnan, Prediction of Boiling and Critical Heat Flux using an Eulerian Multiphase Boiling Model, *Proceedings of the ASME 2010, International Mechanical Engineering Congress & Exposition*, Colorado,USA.

[6] M. Corcione, Empirical correlating equations for predicting the effective thermal conductivity and dynamic viscosity of nanofluids., *Energy Convers. Manage*. 52(1) (2011) 789-793.

[7] M. M. Heyhat, F. Kowsary, A. M. Rashidi, Experimental investigation of laminar convective heat transfer and pressure dropof water-based Al2O3 nanofluids in fully developed flow regime, *Exp. Therm Fluid Sci*, 44(2013) 483–489.

[8] O. S. Prajapati, N. Rohatgi, Flow Boiling Heat Transfer Enhancement by using ZnO-Water Nanofluids". *Science and Technology of Nuclear Installations*, 2014.

[9] A. Atf, A. Rabiee, Enhancement of two phase flow boiling heat transfer in water/Al_2O_3 nanofluid, 2nd *International Conference of Oil, Gas and Petrochemical*, Tehran, Iran, December 2014.

[10] E. Abedinia, T. Zareia, H. Rajabniab, R. Kalbasic, M. Afrandc, Numerical investigation of vapor volume fraction in subcooled flow boiling of a nanofluid, *Journal of Molecular Liuids*, 238(2017) 281-289.

[11] P. Shima, J.Philip, B. Raj, Role of microconvection induced by Brownian motion of nanoparticles in the enhanced thermal conductivity of stable nanofluids". *Appl. Phys. Lett.*; 94 (22)(2009) 223101–223101-3.

[12] W. Evans, J. Fish, P. Keblinski, Role of Brownian motion hydrodynamics on nanofluid thermal conductivity, *Appl. Phys. Lett*. 88 (9)(2006) 093116–093116-3.

[13] N. Kurul, M. Z.Podowski, On the modeling of multidimensional effects in boiling channels, *Proceedings of the* 27th *National Heat Transfer Conference*, Minneapolis, Minnesota, USA, July 1991.

[14] V. H. D. Valle, D. B. R. Kenning, "Subcooled flow boiling at high heat flux, *Int. J. Heat Mass Transfer*, 28(222)(1985) 1907-1920.

[15] R. Cole, A photographic study of pool boiling in the region of the critical heat flux". *AICHE J.*; 6(1960) 533-542.

[16] M. Lemmert, J. M. Chawla, *Influence of flow velocity on surface boiling heat transfer coefficient, Heat Transfer in Boiling*, 237-247.

[17] G. Kocamustafaogullari, M.Ishii, Foundation of the interfacial area transport equation and its closure relations, *Int. J. Heat Mass Transfer*, 38(3)(1995) 481-493.

[18] V. I. Tolubinski, D. M. Kostanchuk, Vapor bubbles growth rate and heat transfer intensity at subcooled water boilin, In: 4th *International Heat Transfer Conference*, Paris, France, 1970.

[19] G. Kocamustafaogullari, M. Ishii,. "Interfacial area and nucleation site density in boiling systems". *Int. J. Heat Mass Transfer*, 26(9)(1983) 1377-1387.

[20] A. Ioilev, et al, *Advances in the modeling of cladding heat transfer and critical heat flux in boiling water reactor fuel assembly*, NURETH-12, Pittsburgh, Pennsylvania, USA. 2007.

[21] A. Tentner, S. Lo, A. Loilev, V. Melnikov, M. Samigulin, V. Ustinenko, V. Kozlov, Advances in computational fluid dynamics modeling of two-phase flow in a boiling water reactor fuel assembly, Proceedings of ICONE14, *Int. Conf. on Nuclear Engineering*, Miami, Florida, July 17-20, 2006.

[22] M. Akbari, N. Galanis, A. Behzadmehr, Comparative assessment of single and two-phase models for numerical studies of nanofluid turbulent forced convection. *Int. J. Heat Fluid Flow*, 37(2012) 136–146.

Please cite this article using:

A. Rabiee and A. Atf, Numerical Investigation of Water/Al_2O_3 Nanofluid Dryout Phenomenon in a Vertical Channel,

AUT J. Mech. Eng., 3(1) (2019) 25-32.

DOI: 10.22060/mej.2017.11920.5555